Chapter 13

Real-Time Detection of Nitric Oxide Release in Live Cells Utilizing Fluorinated Xerogel-Derived Nitric Oxide Sensor

Gi-Ja Lee, Sung Wook Kang, Bochan Seo, Jae Ho Shin and Hun-Kuk Park

Additional information is available at the end of the chapter

http://dx.doi.org/10.5772/60614

Abstract

Nitric oxide (NO) is an important signaling molecule that regulates a diverse range of physiological and cellular processes in many tissues. Therefore, the accurate detection of physiological NO concentration is crucial to the understanding of NO signaling and its biological role. There has been growing interest in the development of electrochemical sensors for direct and real-time monitoring of NO. As the direct electrooxidation of NO requires a relatively high working potential, further surface modification with permselective membranes is required to achieve the desired selectivity for NO via size exclusion or electrostatic repulsion. Here we reported a planar-type NO sensor with a fluorinated xerogel-derived gas permeable membrane for real-time detection of NO release in live cells. First, we evaluated the biocompatibility of xerogel-derived NO permeable membranes modified with fluorinated functional groups by growing RAW 264.7 macrophages on them. And we performed the AFM measurements to examine the morphology of RAW 264.7 macrophages on xerogel membrane. Finally, we successfully detected NO release in RAW 264.7 macrophages, using a planar-type xerogel-derived NO sensor. As a result, fluorinated xerogel-derived membrane could be utilized as both NO permeable and cell-adhesive membranes. Besides, planar-type xerogel-based NO sensors can be easily applied to the cellular sensing system, with a simple coating procedure.

Keywords: Nitric oxide, Live cells, Xerogel, Real-time detection, Cellular sensing

1. Introduction

Nitric oxide (NO) is an important mediator that regulates a diverse range of physiological and cellular processes in many tissues [1,2]. In particular, it plays an important role in a variety of biological processes including neurotransmission, immune defense, regulation of cell death (apoptosis), and cell motility [3–5]. The accurate detection of physiological NO concentration is crucial to the understanding of NO signaling and its biological role. However, it is difficult to accurately measure NO levels in vivo because NO is present at nanomolar concentrations in the body and has a half-life of 2–6 s [6]. Additionally, it is highly reactive with numerous endogenous species including free radicals, peroxides, and oxygen [7,8]. Consequently, most methods for NO detection are indirect including spectroscopic approaches such as the Griess assay for nitrite, detection of nitrate and nitrite with reductase enzymes, and detection of methemoglobin after NO reaction with oxyhemoglobin [9–11]. Unfortunately, these methods often fail to accurately reflect the dynamics of NO in vivo and in real time [12]. Direct measurement strategies are therefore necessary for examining biological process and diseases related to NO in biological conditions, in particular the action of endogenously produced NO.

There has been growing interest in the development of electrochemical sensors for direct and real-time monitoring of NO. Electrochemical methods provide simplicity, fast response times, good sensitivity, high selectivity, and long-term calibration stability [8,12], and thus have significant advantages over other techniques such as electron paramagnetic resonance (EPR) [13–15], chemiluminescence [16–18], and fluorescence [19,20]. As the direct electrooxidation of NO requires a relatively high working potential, further surface modification with permselective membranes is required to achieve the desired selectivity for NO via size exclusion or electrostatic repulsion. Many polymeric materials have been reported as NO-permeable and permselective membranes, including polycarbazole [21], collodion [22], Nafion [23], cellulose acetate [24], poly(tetrafluoroethylene) [25], polydimethylsiloxane (silicone rubber) [26], and multilayer hybrids of these polymers. However, the utility of these polymeric membranes for improving sensor performance *in vivo* or in cells remains limited [8,12].

The sol-gel process is an inorganic polymerization process for the fabrication of materials under mild conditions [27] through the hydrolysis and condensation of suitable alkoxysilane precursors [28]. These sol-gel derived materials (xerogels) have emerged as a class of materials suitable for a wide range of sensing applications [8]. Organically modified xerogels are particularly advantageous for gas sensing applications [29]. The porous inorganic network provides an open and rigid structure for rapid diffusion of gaseous molecules, while the organic groups impart hydrophobicity to the membrane for preventing leakage of the internal electrolyte [30,31]. A previous study reported that sol-gel derived electrochemical sensors showed good sensitivity and selectivity for NO detection in vitro [21,30]. These studies were mainly focused on improving sensor performance such as sensitivity and selectivity, in particular optimization of permselective membrane in vitro.

An amperometric NO sensor for cellular biosensing is significantly affected by the distance between the sensor and the NO-producing cells because NO is rapidly diluted by diffusion under cell-culture conditions [32,33]. However, it is difficult to adjust the exact distance between the needle or disk type sensors and cells without special apparatus [34]. Therefore, it would be better to grow the cells directly on the electrode surface with a NO permeable

http://dx.doi.org/10.5772/60614

membrane. Our previous study reported good sensitivity and selectivity of electrochemical NO sensors with a xerogel membrane in standard solution, but it was mainly focused on membrane optimization including composition, permeability, and contact angle to improve the sensor performance [8,12].

In this study, we developed a planar-type NO sensor with a fluorinated xerogel-derived gas permeable membrane for real-time detection of NO release in live cells including RAW 264.7 macrophages. First, we evaluated the cell viability of RAW 264.7 macrophages on xerogel-derived NO permeable membranes. And we performed the AFM measurement to examine the morphology of RAW 264.7 macrophages on xerogel membrane. Finally, we performed the real-time electrochemical detection of NO release in RAW 264.7 macrophages by lipopolysaccharide (LPS) stimulation utilizing a planar-type NO sensor.

2. Methods used

2.1. Materials

Methyltrimethoxysilane (MTMOS) was purchased from Fluka (Buchs, Switzerland). (Heptadecafluoro-1,1,2,2-tetrahydrodecyl) trimethoxysilane (17FTMS) was purchased from Gelest (Tullytown, PA, USA). Silver and dielectric insulator pastes were purchased from Acheson (Tokyo, Japan) and Jujo (Tokyo, Japan), respectively. Chloroplatinic acid hexahydrate, and lead(II) acetate trihydrate were purchased from Sigma (St. Louis, MO, USA). Nitric oxide (NO; 99.5%), carbon monoxide (CO; 99.5%), and nitrogen (N_2) gases were obtained from Dong-A Scientific (Seoul, South Korea). Other solvents and chemicals were analytical-reagent grade and were used as received. All aqueous solutions were prepared using distilled water of 18.3 MΩ cm resistivity.

2.2. Preparation and biocompatibility test of fluorinated xerogel membrane

A silane solution was prepared by dissolving 18 μL of MTMOS and 4.5 μL of 17FTMS in 727.5 μL of ethanol, as previously reported [12]. The solution was mixed with 160 μL of water, followed by 10μL of HCl (0.5 M) for 1 h. The ensuing solution was deposited on a culture dish and cured for 1 day under ambient conditions.

RAW 264.7 macrophages were cultured in Dulbecco's modified Eagle's medium (DMEM) media with 10% fetal bovine serum (FBS), 1% penicillin, and 1% streptomycin. The cells were then maintained in a humidified atmosphere that contained 5% CO_2 at 37 °C and the medium was changed every second day. Cells were detached by washing and scraping. After washing, cells were resuspended in fresh medium and used for subsequent experiments.

To evaluate the biocompatibility of xerogel membrane, we performed by 3-(4,5-dimethylthiazol- 2-yl)-2,5-diphenyltetrazolium bromide (MTT) assay (Sigma, St.Louis, MO, USA) using RAW 264.7 macrophages. The MTT assay, which is one of the most versatile and popular methods to measure cell viability, involves the conversion of water soluble MTT to an insoluble formazan. The amount of formazan in the MTT assay reflects the total mitochondrial enzymatic

activity of live cells. Cells (1×10^4 cells per well) were seeded in a xerogel membrane coated 96-well plate and incubated for 24, 48, and 72 h. After MTT was added to each group, the cells were incubated for 4 h. The viability was then measured with a microplate reader (Bio-Tek, Winooski, VT, USA) at a test wavelength of 540 nm. The optical density (OD) was calculated as the difference between the reference wavelength and the test wavelength.

2.3. AFM measurement of cells on fluorinated xerogel membrane

RAW 264.7 macrophages on xerogel membrane were characterized using atomic force microscopy (AFM). RAW 264.7 macrophages were washed twice with filtered phosphate buffered saline (PBS, 0.1 M, pH 7.4) and fixed for 20 min in 2.5% glutaraldehyde in PBS at room temperature and 5 ml PBS was added to xerogel-modified culture dish containing fixed cells. Contact mode AFM images were obtained using a NANOS N8 NEOS (Bruker, Herzogenrath, Germany), equipped with a 42.5 μm XY/4 μm Z scanner and a Zeiss optical microscope (Epiplan 500x). The AFM was placed on an active vibration isolation table (TS-150, S.I.S., Herzogenrath, Germany), inside a passive vibration isolation table (Pucotech, Seoul, Korea) to eliminate external noise. Data acquisition and image processing were performed with SPIP (Scanning Probe Image Processor Version 4.1, Image Metrology, Denmark).

Silicon cantilevers with the reflective side coated with gold (Budget Sensor, Bulgaria) were used for the measurements under liquid conditions. The AFM probe tips were stabilized with PBS for at least 10 min prior to scanning. Fixed RAW macrophages were scanned in PBS solution at a resolution of 512 × 512 pixels, at a scan speed of 0.5 line/s.

2.4. Fabrication of planar-type NO sensor

The planar-type NO sensor with three-configuration (i.e., working, reference, and counter electrodes) was prepared using a screen-printing technique, as shown in Figure 1(A). Briefly, a polyester substrate (500 μm thick; 3 M, St. Paul, MN, USA) was thermally treated at 130 °C for 3 h before screen-printing. The silver (for reference electrode and electrical connections), carbon (for working and counter electrodes), and dielectric insulator patterns were sequentially screen-printed onto the thermally pretreated polyester substrate using a LS-150 semi-automated screen printer (Newlong Seimitsu Kogyo; Tokyo, Japan). Each pattern was cured at 130 °C for 13 min. The carbon working electrode (7.1 mm^2) was platinized in 3% chloroplatinic acid hexahydrate and 0.03% lead(II) acetate trihydrate (w/w in water) by cycling the potential from +0.6 to −0.35 V (vs. Ag/AgCl) at a scan rate of 20 mV/s using a CH Instruments 760B bipotentiostat (Austin, TX, USA). The Ag/AgCl reference electrode was prepared by oxidative treatment using 0.3 M $FeCl_3$ solution on the dried silver paste for 15 minutes. A silane solution for xerogel membrane was deposited onto platinized carbon working electrode and allowed to cure for 24 h under ambient conditions.

2.5. Evaluation of planar-type NO sensors

To evaluate the analytical performance of the planar-type NO sensor, amperometric measurements were performed using a CH Instruments 760B bipotentiostat or a portable MicroStat

http://dx.doi.org/10.5772/60614

(Dropsens, Spain). The sensor was prepolarized for 100 min and tested in DMEM solution under ambient conditions with constant stirring. Currents were recorded at an applied potential of +0.8 V (vs. Ag/AgCl). For *in vitro* calibration, a NO standard solution (1.9 mM) was prepared by purging DMEM solution with N_2 gas for 30 min to remove any oxygen, followed by purging with NO (99.5%) for 30 min. The CO solution (0.9 mM) was similarly prepared by consecutively purging DMEM with N_2 for 30 min and CO (99.5%) for another 30 min. (Caution! *The NO and CO purging process must be carried out in a fume hood since NO and CO gases are toxic!*) The solutions of NO and interfering species (nitrite, ascorbic acid, uric acid, acetaminophen, dopamine, hydrogen peroxide, and carbon monoxide) were freshly prepared every second day and stored at 4 °C.

The selectivity of the xerogel-modified sensors for NO in the presence of interfering species was also evaluated using the separate solution method [12], for which the amperometric selectivity coefficients ($\log K_{NO,j}^{amp}$) were calculated using the following equation:

$$\log K_{NO,j}^{amp} = \log\left(\frac{\Delta I_j / c_j}{\Delta I_{NO} / c_{NO}}\right) \quad (1)$$

where ΔI_{NO} and ΔI_j are the measured current values for the target analyte (NO) and interfering species (j = nitrite, ascorbic acid, uric acid, acetaminophen, dopamine, hydrogen peroxide, and carbon monoxide), respectively. The concentration of each interfering substance (c_j) was selected to be 1 μM, the same concentration of NO (c_{NO}).

2.6. Real-time detection of NO release in live cells

RAW 264.7 macrophages (1×10^4 cells/electrode) were grown on top of the electrode surface which was covered with sol–gel-derived membrane. Stimulation of RAW macrophages with LPS (1 μg/ml) was performed after stabilizing the background current for 2~3 h at 37 °C. The experimental scheme is shown in Figure 1(B).

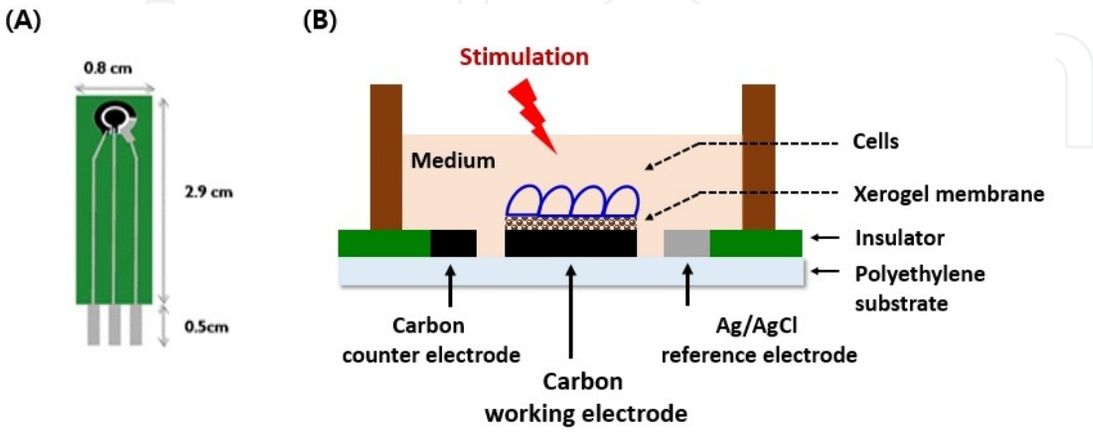

Figure 1. Schematic of (A) screen-printed electrode and (B) experimental design for real-time detection of nitric oxide release in live cells utilizing fluorinated xerogel-derived nitric oxide sensor.

3. Results and discussion

3.1. Cytotoxicity assessment of fluorinated xerogel membrane

In general, amorphous, hydrophobic fluoropolymers are highly permeable to many gaseous species including oxygen, nitric oxide, carbon dioxide, ammonia, and volatile organic compounds [12,35]. Indeed, a microporous poly(tetrafluoroethylene) (PTFE) film has been extensively employed to improve a Clark-type oxygen sensor as a gas-permeable membrane [36,37]. The PTFE membrane effectively prevented the biofouling at the interface between the sensor surface and the biological samples (e.g., blood), while enabling high permeation and rapid diffusion of oxygen [36]. However, the fabrication of such sensors remains complicated. The PTFE film must be stretched across the electrode and fixed to the sensor. This process is often irreproducible, impacting both the thickness of the gas-permeable membrane and the sensor's response to oxygen [29,36].

In this study, we employed a fluorinated xerogel gas-permeable membrane to take advantage of both the versatility of sol–gel chemistry and high and fast gas permselectivity like PTFE. Our previous study reported good sensitivity and selectivity of electrochemical NO sensors with a xerogel membrane in standard solution [8,12]. In addition, we had preliminarily evaluated the cell viability, adhesion, and growth of cells on xerogel-derived NO permeable membrane, comparing with that of other cell-adhesive matrices such as collagen and poly L-lysine [34].

Here, we performed an MTT assay to reconfirm the cytotoxicity of fluorinated xerogel-derived NO permeable membrane, prior to real-time detection of NO release in live cells. RAW 264.7 macrophages were incubated on fluorinated xerogel-derived NO permeable membrane and collagen for 24, 48, and 72 h. Similar to preliminary result, the viability of RAW 264.7 cells exposed to xerogel membrane for 24 h was 102.64 ± 3.52%. This result showed that fluorinated xerogel-derived NO permeable membrane was not cytotoxic to RAW 264.7 macrophages. Moreover, the proliferation of RAW 264.7 macrophages was not influenced during 48 and 72 h of growth on the xerogel membrane.

3.2. Morphology of RAW macrophages on fluorinated xerogel membrane

Macrophages, which was derived from circulating blood monocytes and reside in most tissues, play an important role in host defense and tissue homeostasis as they ingest dead tissue and fight invading pathogens [38,39]. Therefore, the activation of macrophages is a general characteristic for the early stages of pathogens infection. LPS, a major outer membrane component of Gram-negative bacteria, plays an important role in the pathogenesis of Gram-negative bacterial infection [40] and has been served as an important active component for pathogen-induced macrophage inflammation studies [41]. In general, LPS stimulation caused some morphological changes in human macrophages such as the formation of lamellipodia and the extensive cell spreading [42]. But these LPS induced morphological changes in RAW 264.7 macrophages by conventional microscopy could not provide the ultrastructural changes in RAW 264.7 macrophages by LPS stimulation.

http://dx.doi.org/10.5772/60614

AFM has emerged as an imaging technique that provides 3D topographic information and structural details of biological samples including microorganisms, cell membranes, biopolymers, and more. Therefore, AFM is now a common tool for nanotechnology, not only for imaging but also to measure the interaction forces in biological systems [43]. We performed AFM measurement to observe the morphological changes in RAW macrophages on xerogel membrane following LPS treatment. Figure 2 shows representative AFM 3D topography images taken from LPS-stimulated RAW cells for 0, 0.5, 1, 1.5, 6, and 24 h. As shown in Figure 2(A), control RAW macrophage showed a typical spherical shapes with ruffled membranes and a few lamellipodia surround them. But the morphology of RAW cells after 1 h LPS stimulation exhibited the extension of the cytoplasm toward its outside, as shown in Figure 2(C). After the LPS exposure for 1.5 h, they appeared spindle and long-stretched shapes (Figure 2(D)). The number of microspikes was increased from 1.5 h after stimulation of LPS. As a result, RAW macrophages for 24 h LPS stimulation showed strong lamellipodia with a lot of dendritic pseudopod. In addition, LPS stimulated RAW macrophages for 24 h showed some holes on their surface. Saxena et al. [44] reported that LPS induced differentiation of RAW 264.7 macrophage cells into dendritic like cells. And Pi et al. [39] reported the LPS activated RAW 264.7 macrophages changed to be much bigger than control cells with some holes emerged on cell surface. From AFM results, we suggested that RAW macrophages on fluorinated xerogel-derived NO permeable membrane were normally activated by LPS stimulation.

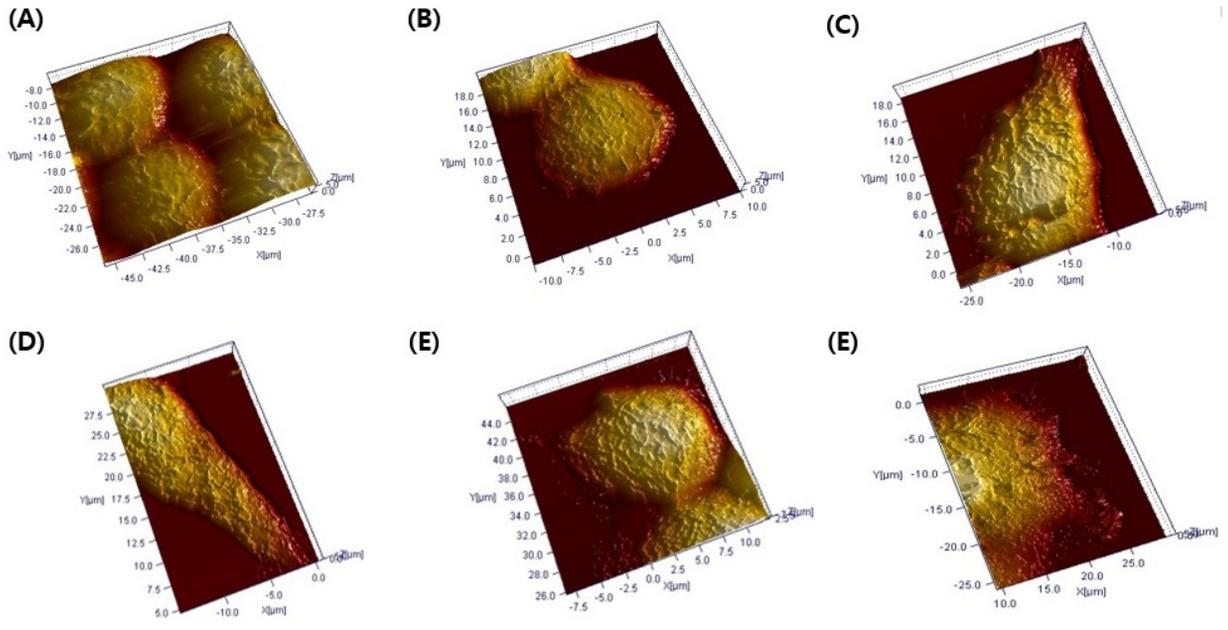

Figure 2. Representative AFM 3D topography images of RAW 264.7 macrophages on fluorinated xerogel-membrane after LPS (1 μg/ml) stimulation for (A) 0, (B) 0.5, (C) 1, (D) 1.5, (E) 6, and (F) 24 h.

3.3. Amperometric response of xerogel-derived planar-type NO sensor

The sensor performance of the resulting NO microelectrode was investigated in DMEM solution. The calibration and dynamic response curves for NO and interfering species (i.e.,

nitrite) are shown in Figure 3. A sensor coated with fluorinated xerogel membrane did not exhibit serious interference from nitrite concentrations of up to 20 μM, which is a concentration much greater than the highest level present in physiological samples. Indeed, the fluorinated xerogel-modified sensors exhibited excellent selectivity ($\log K_{NO,j}^{amp}$) of < –5, <–5, <–5, <–5, <–5, –4.38, and –3.85 for *j* = nitrite, ascorbic acid, uric acid, acetaminophen, dopamine, hydrogen peroxide, and carbon monoxide, respectively. In addition, the xerogel-derived sensor responded to NO concentrations of up to 1,000 nM with respect to sensitivity (0.15 ± 0.012 nA/nM), linearity (R^2 = 0.9981, 20~1,000 nM NO range), and response time ($t_{90\%}$ < 10 s).

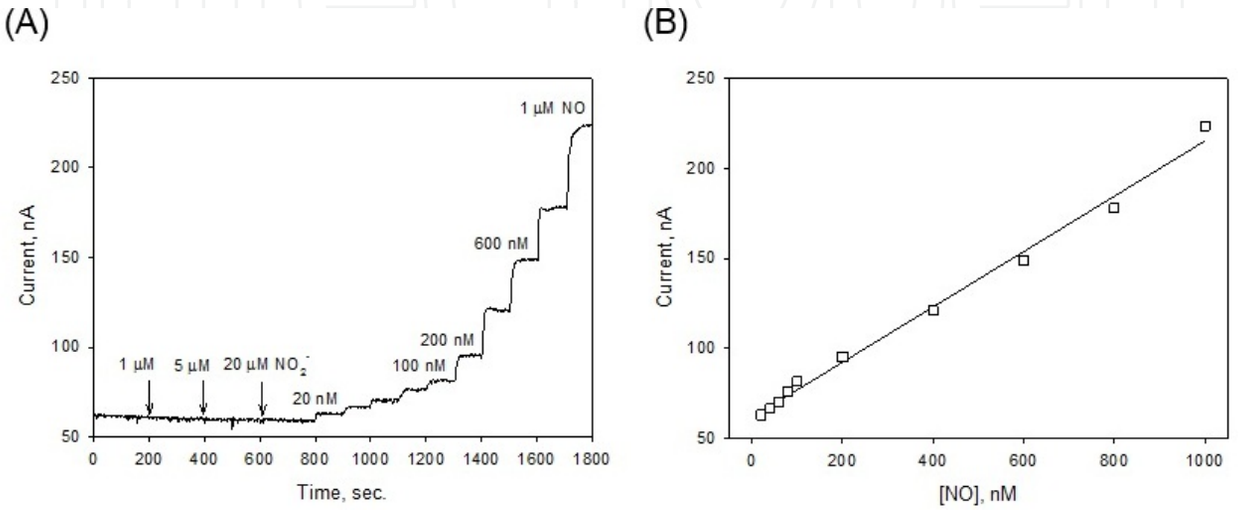

Figure 3. Dynamic response (A) to nitric oxide and an interfering species (nitrite) and calibration curve (B) of the nitric oxide sensor modified with fluorinated xerogel-derived membrane.

3.4. Real-time detection of NO release in live cells utilizing planar-type NO sensor

NO plays an important role in a variety of cellular functions, including blood vessel relaxation, neurotransmission, and immune response [34]. It is produced through the conversion of L-arginine into L-citrulline by diverse cell types such as macrophages, neutrophils, neuronal cells, and endothelial cells as both an extra and intracellular signaling molecule [45]. The mechanisms of NO formation by three kinds of nitric oxide synthase (NOS), including endothelial (eNOS), neuronal (nNOS), and inducible NOS (iNOS), are well established [46]. Among them, the expression of iNOS is induced by stimulation of cells with LPS and/or proinflammatory cytokines [46,47]. Macrophage iNOS is responsible for producing large quantities of NO, which are synthesized over the period of several hours after cells are stimulated [34]. NO plays an important role as part of a nonspecific defense mechanism, as a signaling molecule between macrophages and other cells and as an intracellular messenger within the macrophages themselves [45]. Besides, NO produced by endothelium cells plays a critical role in regulation of vascular tone and activity. The continuous detection of NO release from endothelium could provide new and important insights into the modulatory role of NO in cardiovascular system [48].

However, most methods for NO quantification are indirect including spectroscopic approaches such as the Griess assay which determines the major and stable products of NO

http://dx.doi.org/10.5772/60614

degradation—nitrite and nitrate, as well as the detection of methemoglobin after NO reaction with oxyhemoglobin [9–11]. Unfortunately, these methods often fail to accurately reflect the dynamics of NO *in vivo*, *in vitro*, and in real time [12]. In contrast to other electrochemical NO sensor designs, xerogel-based NO sensors are fabricated using a simple coating procedure, with high sensitivity, selectivity, and reproducibility [8].

Figure 4 represents real-time detection monitoring of NO release by a planar-type xerogel-derived NO sensor in RAW 264.7 macrophages stimulated by LPS. In control RAW macrophages, there was no increase in current throughout the whole experimental period. But the current resulting from NO production started to rise in 5,500 s after LPS stimulation. After reaching the maximum current in 6,000 s, a slow decline in NO production lasted for the rest of the experiment. The maximum change in NO concentration was about 60 nM, based on *in vitro* calibration results.

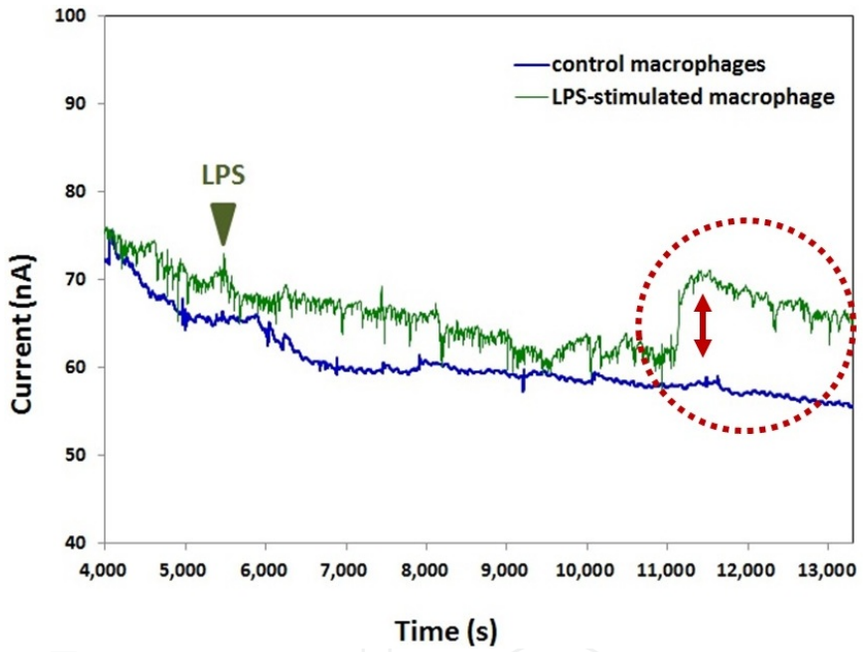

Figure 4. Representative real-time measurement of NO release in RAW 264.7 macrophages stimulated by lipopolysaccharide.

4. Conclusions

In this study, we evaluated the biocompatibility of sol-gel derived NO permeable membranes modified with fluorinated functional groups with RAW 264.7 macrophages. Our results showed that xerogel-derived NO permeable membrane was nontoxic and could provide good cell adhesion. In addition, the morphology of these adhering RAW 264.7 macrophages did not show any differences compared to those grown on other biocompatible membranes. Therefore, we expected that fluorinated xerogel-derived membrane could be utilized as both NO gas

permeable and cell-adhesive membranes on which cells are directly grown for a cellular NO sensor. Besides, in the planar-type sensor with NO permeable membrane, there is no need to adjust the distance between sensor and cells. Overall, in contrast to other electrochemical NO sensor designs, xerogel-based NO sensors can be easily applied to the cellular sensing system, with a simple coating procedure.

In summary, a planar-type NO sensor with fluorinated xerogel membrane has good sensitivity and specificity for detecting biologically released NO in live cells. And we successfully measured the NO release in RAW 264.7 macrophages stimulated by LPS, utilizing our planar-type xerogel-derived NO sensor. Therefore, we expect that our sensor can be applied for real-time monitoring of NO dynamics in various cells, tissues, and organs.

Acknowledgements

This study was supported by the National Research Foundation of Korea (NRF) funded by the Ministry of Science, ICT & Future Planning (2010-0019917), and the Ministry of Education (2013R1A1A2065149).

Author details

Gi-Ja Lee[1,2], Sung Wook Kang[1], Bochan Seo[3], Jae Ho Shin[3] and Hun-Kuk Park[1,2*]

*Address all correspondence to: sigmoidus@khu.ac.kr

1 Department of Biomedical Engineering & Healthcare Industry Research Institute, College of Medicine, Kyung Hee University, Seoul, Korea

2 Department of Medical Engineering, Graduate School, Kyung Hee University, Seoul, Korea

3 Department of Chemistry, College of Natural Science, Kwangwoon University, Seoul, Korea

References

[1] Brown FO, Finnerty NJ, Lowry JP. Nitric oxide monitoring in brain extracellular fluid: Characterisation of Nafion-modified Pt electrodes *in vitro* and *in vivo*. Analyst. 2009;134:2012–2020. DOI: 10.1039/B909005C

[2] Deng XD, Wang F, Chen Z. A novel electrochemical sensor based on nano-structured film electrode for monitoring nitric oxide in living tissues. Talanta. 2010;82:1218–1224. DOI: 10.1016/j.talanta.2010.06.035

[3] Hibbs JB, Taintor RR, Vavrin Z, Rachelin EM. Nitric oxide: A cytotoxic activated macrophage effector molecule. Biochem. Biophys. Res. Commun. 1988;157:87–94. DOI: 10.1016/S0006-291X(88)80015-9

[4] Palmer PMJ, Ferrige AG, Moncada S. Nitric oxide release accounts for the biological activity of endothelium-derived relaxing factor. 1987;327:524–526. DOI: 10.1038/327524a0

[5] Szabo C. Physiological and pathophysiological roles of nitric oxide in the central nervous system. Brain Res. Bull. 1996;44:131–141. DOI: 10.1016/0361-9230(96)00159-1

[6] Lee GJ, Chae SJ, Kim SK, Lee S, Shin JH, Kim W, Park HK. Real time dynamics of nitric oxide during cardiac ischemia-reperfusion of the rat. Sens. Actuators B Chem. 2012;161:480–485. DOI: 10.1016/j.snb.2011.10.064

[7] Bedioui F, Trevin S, Devynck J. Chemically modified microelectrodes designed for the electrochemical determination of nitric oxide in biological systems. Electroanalysis. 1996;8:1085–1091. DOI: 10.1002/elan.1140081202

[8] Shin JH, Weinman SW, Schoenfisch MH. Sol-gel derived amperometric nitric oxide microsensor. Anal. Chem. 2005;77:3494–3501. DOI: 10.1021/ac048153i

[9] Archer S. Measurement of nitric oxide in biological models. FASEB J. 1993;7:349–360. DOI: 0892-6638/93/0007-0349

[10] Taha TH. Nitric oxide measurements in biological samples. Talanta. 2003;61:3–10. DOI: 10.1016/S0039-9140(03)00354-0

[11] Wang Y, Hu S. Nitric oxide sensor based on poly (p-phenylenevinylene) derivative modified electrode and its application in rat heart. Bioelectrochemistry. 2009;74:301–305. DOI: 10.1016/j.bioelechem.2008.11.002

[12] Shin JH, Privett BJ, Kita JM, Wightman RM, Schoenfisch MH. Fluorinated xerogel-derived microelectrodes for amperometric nitric oxide sensing. Anal. Chem. 2008;80:6850–6859. DOI: 10.1021/ac800185x

[13] Fujii S, Yoshimura T. A new trend in iron–dithiocarbamate complexes: as an endogenous NO trapping agent. Coord. Chem. Rev. 2000;198:89–99. DOI: 10.1016/S0010-8545(99)00196-4

[14] Han TH, Hyduke DR, Vaughn MW, Fukuto JM, Liao JC. Nitric oxide reaction with red blood cells and hemoglobin under heterogeneous conditions. PNAS. 2002;99:7763–7768. DOI: 10.1073/pnas.122118299

[15] Takahashi S, Omori Y, Miyazaki H, Yoshino F, Shoji H, Lee MC, Todoki K, Kamibayashi M, Murakami E. Real-time monitoring of nitric oxide in ischemic myocardium using an NO-selective electrode calibrated by electron spin resonance. Life Sci. 2003;74:75–85. DOI: 10.1016/j.lfs.2003.06.027

[16] Kikuchi K, Nagano T, Hayakawa H, Hirata Y, Hirobe M. Detection of nitric oxide production from a perfused organ by a luminol-hydrogen peroxide system. Anal. Chem. 1993;65:1794–1799. DOI: 10.1021/ac00061a025

[17] Kikuchi K, Nagano T, Hayakawa H, Hirata Y, Hirobe M. Real time measurement of nitric oxide produced ex vivo by luminol-H_2O_2 chemiluminescence method. J. Biol. Chem. 1993;268:23106–23110 / 8226828.

[18] Robinson JK, Bollinger MJ, Birks JW. Luminol/H_2O_2 chemiluminescence detector for the analysis of nitric oxide in exhaled breath. Anal. Chem. 1999;71:5131–5136. DOI: 10.1021/ac990646d

[19] Gabe Y, Urano Y, Kikuchi K, Kojima H, Nagano T. Highly sensitive fluorescence probes for nitric oxide based on boron dipyrromethene chromophore-rational design of potentially useful bioimaging fluorescence probe. J. Am. Chem. Soc. 2004;126:3357–3367. DOI: 10.1021/ja037944j

[20] Kojima H, Nakatsubo N, Kikuchi K, Kawahara S, Kirino Y, Nagoshi H, Hirata Y, Nagano T. Detection and imaging of nitric oxide with novel fluorescent indicators: Diaminofluoresceins. Anal Chem. 1998;70:2446–2453. DOI: 10.1021/ac9801723

[21] Prakash R. Srivastava RC, Seth PK. Polycarbazole modified electrode; nitric oxide sensor. Polym. Bull. 2001;46:487–490. DOI: 10.1007/s002890170036

[22] Kitamura Y, Uzawa T, Oka K, Komai Y, Takizawa N, Kobayashi H, Tanishita K. Operation of a miniature redox hydrogel-based pyruvate sensor in undiluted deoxygenated calf serum. Anal. Chem. 2000;72:2957–2968. DOI: 10.1021/ac991021i

[23] Zhang X, Cardosa L, Broderick M, Fein H, Lin J. An integrated nitric oxide sensor based on carbon fiber coated with selective membranes. Electroanalysis. 2000;12:1113–1117. DOI: 10.1002/1521-4109(200010)

[24] Cserey A, Gratzl M. Stationary-state oxidized platinum microsensor for selective and on-line monitoring of nitric oxide in biological preparations. Anal. Chem. 2001;73:3965–3974. DOI: 10.1021/ac010123h

[25] Lee Y, Oh BK, Meyerhoff ME. Improved planar amperometric nitric oxide sensor based on platinized platinum anode. 1. Experimental results and theory when applied for monitoring NO release from diazeniumdiolate-doped polymeric films. Anal. Chem. 2004;76:536–544. DOI: 10.1021/ac035064h

[26] Mizutani F, Hirata Y, Yabuki S, Iijima S. Amperometric measurement of nitric oxide (NO) using an electrode coated with polydimethylsiloxane. Chem. Lett. 2000;29:802–803. DOI: 10.1246/cl.2000.802

[27] Coradin T, Boissiere M, Livage J. Sol-gel chemistry in medicinal science. Curr. Med. Chem. 2006;13:99–108. DOI: 10.2174/092986706789803044

[28] Islamnezhad A, Valizadeh M. Taguchi OA25 orthogonal array design for the optimization of La^{3+}-selective electrode prepared by sol-gel technique. Anal. Bioanal. Electrochem. 2012;4:386–398.

[29] Lee GJ, Kim SK, Kang SW, Kim OK, Chae SJ, Choi S, Shin JH, Park HK, Chung JH. Real time measurement of myocardial oxygen dynamics during cardiac ischemia-reperfusion of rats. Analyst. 2012;137:5312–5319. DOI: 10.1039/c2an35208g

[30] Tsionsky M, Lev O. Electrochemical composite carbon-ceramic gas sensors: introduction and oxygen sensing. Anal. Chem. 1995;67:2409–2414. DOI: 10.1021/ac00110a014

[31] Rabinovich L, Lev O, Tsirlina GA. Electrochemical characterisation of Pd modified ceramic / carbon electrodes: Partially flooded versus wetted channel hydrophobic gas electrodes. J. Electroanal. Chem. 1999;466:45–59. DOI: 10.1016/S0022-0728(99)00118-7

[32] Asakawa H, Mochitate K, Haruyama T. Seamless signal transduction from live cells to an NO Sensor via a cell-adhesive sensing matrix. Anal. Chem. 2008;80:1505–1511. DOI: 10.1021/ac702001u

[33] Isik S, Etienne M, Oni J, Blochl A, Reiter S, Schuhmann W. Dual microelectrodes for distance control and detection of nitric oxide from endothelial cells by means of scanning electrochemical microscope. Anal. Chem. 2004;76:6389–6394. DOI: 10.1021/ac049182w

[34] Kang SW, Seo B, Kim JH, Kim OK, Shin JH, Lee GJ, Park HK. Cell viability, adhesion and function of RAW 264.7 macrophages on fluorinated xerogel-derived nitric oxide permeable membrane for the application of cellular sensing. J. Nanosci. Nanotechnol. 2014;14:8398–8404. DOI: 10.1166/jnn.2014.9928

[35] Moskvin LN, Nikitina TG. Membrane methods of substance separation in analytical chemistry. J. Anal. Chem. 2004;59:2–16. DOI: 10.1023/B:JANC.0000011661.47796.b2

[36] Park SS, Hong M, Song CK, Jhon GJ, Lee Y, Suh M. Real-time in vivo simultaneous measurements of nitric oxide and oxygen using an amperometric dual microsensor. Anal. Chem. 2010;82:7618–7624. DOI: 10.1021/ac1013496

[37] Wang Z, Lin P, Baker GA, Stetter J, Zeng X. Ionic liquids as electrolytes for the development of a robust amperometric oxygen sensor. Anal. Chem. 2011;83:7066–7073. DOI: 10.1021/ac201235w

[38] Murray PJ, Wynn TA. Protective and pathogenic functions of macrophage subsets. Nat. Rev. Immunol. 2011;11:723–737. DOI: 10.1038/nri3073

[39] Pi J, Li T, Liu J, Su X, Wang R, Yang F, Bai H, Jin H, Cai J. Detection of lipopolysaccharide induced inflammatory responses in RAW 264.7 macrophages using atomic force microscope. Micron. 2014;65:1–9. DOI: 10.1016/j.micron.2014.03.012

[40] Khan SA, Everest P, Servos S, Foxwell N, Zahringer U, Brade H, Rietschel ET, Dougan G, Charles IG, Maskell DJ. A lethal role for lipid A in Salmonella infections. Mol. Microbiol. 1998;29:571–579. DOI: 10.1046/j.1365-2958.1998.00952.x

[41] Smith PD, Smythies LE, Mosteller-Barnum M, Sibley DA, Russell MW, Merger M, Sellers MT, Orenstein JM, Shimada T, Graham MF, Kuba-gawa H. Intestinal macrophages lack CD14 and CD89 and consequently are down-regulated for LPS- and IgA-mediated activities. J. Immunol. 2001;167:2651–2656. DOI: 10.4049/jimmunol.167.5.2651

[42] Williams LM, Ridley AJ. Lipopolysaccharide induces actin reorganization and tyrosine phosphorylation of Pyk2 and paxillin in monocytes and macrophages. J. Immunol. 2000;164:2028–2036. DOI: 10.4049/jimmunol.164.4.2028

[43] Choi S, Jung GB, Kim KS, Lee GJ, Park HK. Medical applications of atomic force microscopy and raman spectroscopy. J. Nanosci. Nanotechnol. 2014;14:71–97. DOI: 10.1166/jnn.2014.9112

[44] Saxena RK, Vallyathan V, Lewis DM. Evidence for lipopolysaccharide-induced differentiation of RAW 264.7 murine macrophage cell line into dendriticlike cells. J. Biosci. 2003;28:129–134. DOI: 10.1007/BF02970143

[45] Pekarova M, Kralova J, Kubala L, Ciz M, Lojek A, Gregor C, Hrbac J. Continuous electrochemical monitoring of nitric oxide production in murine macrophage cell line RAW 264.7. Anal. Bioanal. Chem. 2009;394:1497–1504. DOI: 10.1007/s00216-009-2813-x

[46] Mayer B, Hemmens B. Biosynthesis and action of nitric oxide in mammalian cells. Trends Biochem. Sci. 1997;22:477–481. DOI: 10.1016/S0968-0004(97)01147-X

[47] Yao D, Vlessidis AG, Evmiridis NP. Determination of nitric oxide in biological samples. Microchim. Acta. 2004;147:1–20. DOI: 10.1007/s00604-004-0212-8

[48] Du F, Huang W, Shi Y, Wang Z, Cheng J. Real-time monitoring of NO release from single cells using carbon fiber microdisk electrodes modified with single-walled carbon nanotubes. Biosens. Bioelectron. 2008;24:415–421. DOI: 10.1016/j.bios.2008.04.020